

automation, control, tower cranes

**Wojciech SOLARZ, Grzegorz TORA\***

Cracow University of Technology, Institute of Machine Design

Al. Jana Pawła II 37, 31-864 Kraków, Poland

\**Corresponding author.* E-mail: tora@mech.pk.edu.pl

## SIMULATION OF CONTROL DRIVES IN A TOWER CRANE

**Summary.** The design of a control system for a tower crane is investigated. Underlying the controller design is the theory of optimal linear control. Computer models of a crane and the control systems for the crane drives are developed. Simulation data reveals that the motion of the load can be effectively controlled so that it should follow a predetermined trajectory.

## SYMULACJA STEROWANIA NAPĘDAMI ŻURAWIA WIEŻOWEGO

**Streszczenie.** Artykuł przedstawia budowę układu sterowania żurawia wieżowego. W regulatorze układu wykorzystano teorię optymalnej regulacji liniowej. Zbudowano komputerowe modele żurawia oraz układu regulacji napędów. Na podstawie symulacji wykazano, że można efektywnie sterować ruchem ładunku żurawia zgodnie z założoną trajektorią.

### 1. INTRODUCTION

Dynamic processes tend to disturb crane operations, causing the sway of the load suspended on ropes, which negatively impacts on the accuracy of position control and work safety [12]. It is most desirable to eliminate the sway in the final phase of load motion. Such strategy is adopted by experienced crane operators, who carefully select the drives to be applied, though in order to entirely eliminate the load sway, it is required that a control system be incorporated in the crane structure.

Input shaping is a widely adopted control scheme for automatic elimination of swaying of the payload being handled [1, 8, 9, 15]. Real-time estimations of natural frequencies and damping ratios yield the input shaper implemented in the crane drives. The convolution of the main control signal and input shaper signals creates a command signal to control the crane. The method has been successfully applied not only in tower cranes, but in gantry cranes and in level lifting jib cranes. Another method of sway reduction works by implementing the pre-planned lifting path using a feedback controller based on a nonlinear kinematic and dynamic model of the crane, taking into account the drive constraints [2, 16]. The feedback controller requires the online measurements of displacements of the drives and of payload position within the crane's working space. The payload position can be measured directly with laser sensors [10], though these are difficult to use at nights, in the rain and in dusty environments. The indirect method involves the measurements of hoisting rope position and two swing angles. Application of two transversely arranged rotary frames encompassing the hoisting rope and suspended under the trolley enables the measurement of the swing angles using encoders fitted to the frame axes. [7, 14]. The optimised trajectory connecting the start and end position of the payload can be derived, the typical optimisation criterion being the minimal handling

time. A major drawback, however, is that the initial conditions have to be first determined and real time calculations of the entire trajectory are required, which becomes a cumbersome procedure [3], [12, 14]. The design of the payload path has to take into account the presence of other objects and structures on the construction site [6]. In order to precisely design the payload path it is required that crane and drive flexibility should be taken into account [5]. Application of the dynamic model of the crane taking into account the flexibility features vastly complicates the calculation procedure. An important contribution to the study of vibration reduction methods is offered by experimental programs carried out in laboratory conditions allowing the methods to be verified and improved at relatively low costs [9, 11, 15]. This study utilises the crane control strategy aimed to generate the optimised trajectory of the payload to be handled. Apart from the starting point and the initial velocity, the parameters that are known include the end position of the payload, so the path can be assumed in between and the velocity along the path can be found [13]. The mathematical expression of the trajectory enables the calculation of the instantaneous payload acceleration. The inertia and gravity forces acting upon the payload yield the resultant force tensioning the hoisting rope. The direction of this force determines the instantaneous values of the distance between the jib and the trolley, the angular position of the jib, the rope length and the swaying angles. These parameters need to be known in order to fabricate the feedback controller.

## 2. INVERSE PROBLEM OF THE TOWER CRANE KINEMATICS

The inverse problem of kinematics involves finding the displacements of the crane drives and their derivatives, as well as swaying angles for the pre-planned velocity along the payload travel path. Full implementation of the drive control should take into account those factors that have a major bearing on the travel path:

- a) jib rotation drive, trolley travel drive, rope winding drive,
- b) deformations of the tower, jib and hoisting rope under the applied loading,
- c) drive flexibility, considering the mass of hoisting rope and the rope hoisting,
- d) wind.

In the first stage the crane model is developed that takes into account the aspect (a) only. Results will be utilised as baseline data for further research work on an extended model of the crane, taking into account the other listed factors. In the context of the assumption that the hoisting rope should be weightless, inextensible and flabby, the hoisting rope will always have the direction of the tensioning force, being the resultant of the forces acting upon the payload's centre of gravity (further referred to just as the payload), as shown in Fig. 1:

$$F_p \mathbf{f}^o = m_p (\mathbf{g} - \mathbf{a}_p) \quad (1)$$

where:

$m_p$  - payload mass,

$\mathbf{a}_p$  - vector of payload's acceleration;

$\mathbf{g}$  - vector of gravity's acceleration.

Eq (1) yields the value of the tensioning force:

$$F_p = m_p \|\mathbf{g} - \mathbf{a}_p\| \quad (2)$$

and the versor of the tensioning force direction:

$$\mathbf{f}^o = \frac{\mathbf{g} - \mathbf{a}_p}{\|\mathbf{g} - \mathbf{a}_p\|} \quad (3)$$

The trajectory is obtained by finding the radius vector of the payload associated with  $s$  - payload displacement along the travel path:  $\mathbf{r}_p = [x_p(s), y_p(s), z_p(s)]$ , for the given velocity pattern of the payload motion along this path:

$$\frac{ds}{dt} = \dot{s} = v_p(s) \quad (4)$$

where:  $v_p(s) > 0$ ,  $v_p(0) = 0$ ,  $v_p(S) = 0$ ,  $S$  - length of the travel path.

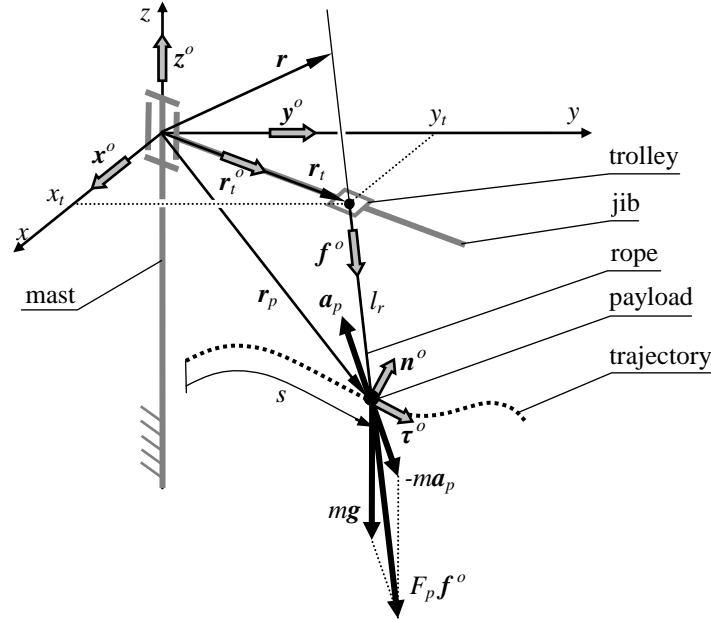


Fig. 1. Force vectors and directional versors of the tower crane  
Rys. 1. Wektory sił i wersory kierunkowe żurawia wieżowego

The total time of payload motion becomes:

$$T = \int_0^S \frac{ds}{v_p(s)} \quad (5)$$

The acceleration vector is associated with the assumed trajectory:

$$\mathbf{a}_p = s \boldsymbol{\tau}^o + s^2 k \mathbf{n}^o \quad (6)$$

where:

$$s = \frac{dv_p}{ds} v_p, \quad \boldsymbol{\tau}^o = \frac{d\mathbf{r}_p(s)}{ds} \text{ - versor tangent to the travel path,}$$

$$\mathbf{n}^o = \frac{1}{k} \frac{d^2 \mathbf{r}_p(s)}{ds^2} \text{ - versor normal to the travel path,}$$

$$k = \left\| \frac{d^2 \mathbf{r}_p(s)}{ds^2} \right\| \text{ - path curvature.}$$

The trolley can assume the position defined by the radius vector lying in the plane described by the jib:

$$\mathbf{r}_t = x_t \mathbf{x}^o + y_t \mathbf{y}^o + 0 \mathbf{z}^o \quad (7)$$

where:

$x_t, y_t, z_t = 0$  - trolley coordinates in the plane described by the jib,

$\mathbf{x}^o, \mathbf{y}^o, \mathbf{z}^o$  - versors of the axis in the immobile reference system.

The equation of the radius vector of the straight line along which the hoisting rope is stretched is given as:

$$\mathbf{r} = \mathbf{r}_p + \mathbf{f}^o f \quad (8)$$

where:  $f \in R$  - parameter expressed in the unit of length.

The trace of a line along which the hoisting rope stretches itself on the plane described the jib determines the trolley position. Solving the system of equations (7) and (8) in terms of:  $x_t$ ,  $y_t$  and  $f$  yields:

$$\mathbf{r}_t = \mathbf{r} \rightarrow x_t \mathbf{x}^o + y_t \mathbf{y}^o = \mathbf{r}_p + \mathbf{f}^o f \quad (9)$$

Projecting the vectors given in Eq (9) onto the directions of versors in the immobile reference system yields:

$$x_t = (\mathbf{r}_p + \mathbf{f}^o f) \cdot \mathbf{x}^o, \quad y_t = (\mathbf{r}_p + \mathbf{f}^o f) \cdot \mathbf{y}^o, \quad f = -\frac{\mathbf{r}_p \cdot \mathbf{z}^o}{\mathbf{f}^o \cdot \mathbf{z}^o} \quad (10)$$

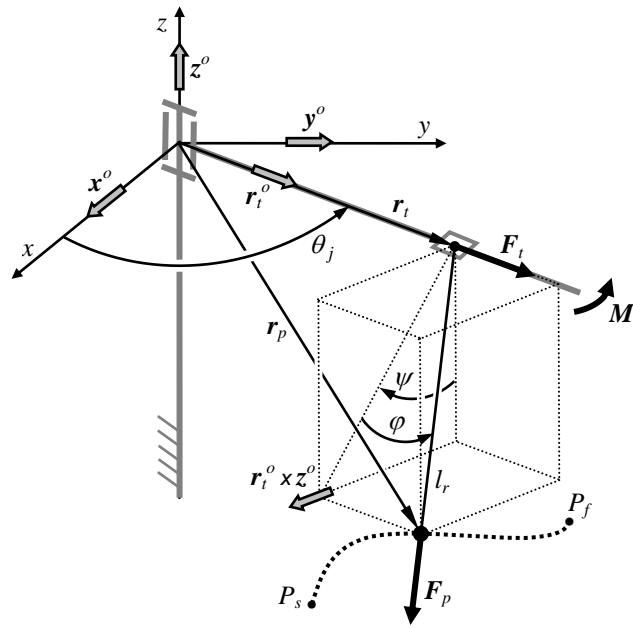


Fig. 2. Swing angles and loading of the crane drives

Rys. 2. Kąty wychylenia liny z ładunkiem od pionu i obciążenia napędów żurawia wieżowego

The instantaneous hoisting rope length becomes:

$$l_r = |f| \quad (11)$$

The distance between the trolley and the tower mast axis is expressed as:

$$r_t = \|\mathbf{x}_t \mathbf{x}^o + y_t \mathbf{y}^o\| \quad (12)$$

The angle of jib rotation becomes:

$$\theta_j = \text{sign}(y_t) \arccos(\mathbf{r}_t^o \cdot \mathbf{x}^o) \quad (13)$$

where:  $\mathbf{r}_t^o = \frac{\mathbf{r}_t}{r_t}$  - versor in the direction of the jib.

Swing angles:

$$\varphi_r = \arcsin\left(\frac{(\mathbf{r}_p - \mathbf{r}_t) \cdot \mathbf{r}_t^o}{l_r}\right), \quad \psi_r = -\arctan\left(\frac{\mathbf{r}_p \cdot (\mathbf{r}_t^o \times \mathbf{z}^o)}{\mathbf{r}_p \cdot \mathbf{z}^o}\right) \quad (14)$$

Finding  $\theta_j, r_t, l_r, \varphi_r, \psi_r$  in the explicit form (see Fig. 2) completes the inverse problem of kinematics of the tower crane in terms of displacement and their respective derivatives can be now calculated.

### 3. INVERSE PROBLEM OF THE TOWER CRANE DYNAMICS

The inverse problem of dynamics consists in finding the drives loading in the tower crane, which appears when the pre-planned trajectory is to be realise. The force generated on the drum of the winding installation is derived from formula (2). The rope tensioning force that holds the trolley in position, the trolley being treated as a particle, is expressed as:

$$\mathbf{F}_t = (\mathbf{F}_p \cdot \mathbf{r}_t^o - m_t r - m_t r_t \theta_j^2) \mathbf{r}_t^o \quad (15)$$

where:  $m_t$  - mass of the trolley.

Torque transmitted by the jib swing becomes:

$$\mathbf{M}_j = [(\mathbf{r}_t^o \times \mathbf{F}_p) \cdot \mathbf{z}^o - J_{jz} \theta_j - 2m_t r_t \theta_j] \cdot \mathbf{z}^o \quad (16)$$

where:

$J_{jz}$  - mass moment of jib's inertia computed round the vertical axis in the immobile coordinate system.

### 4. CONTROL SYSTEM

Underlying the synthesis of the control system (Fig. 3.) are the following assumptions: crane elements are taken as rigid, ropes are taken as rigid and weightless, the load is treated as a particle, the motion of a load suspended on ropes is treated as that of a spherical pendulum, no friction, the drives execute the required torque in an ideal manner.

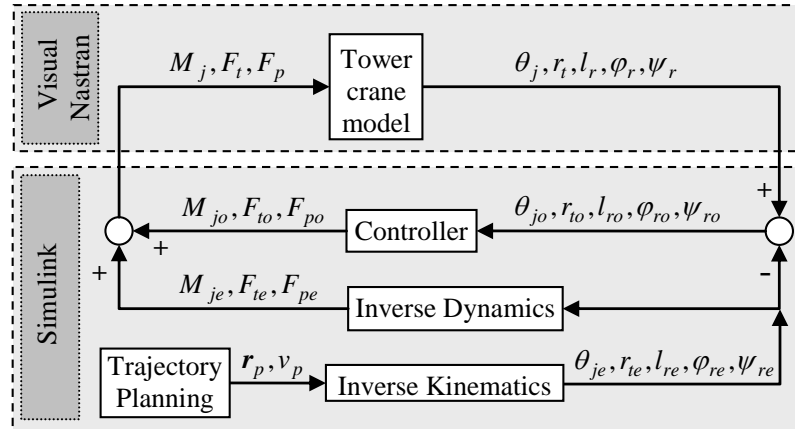


Fig. 3. Model of a tower crane and control system

Rys. 3. Model układu sterowania żurawia wieżowego

Basing on the pre-planned travel path  $r_p(s)$  and the assumed velocity pattern  $v_p(s)$ , the Inverse Kinematics block yields the predicted values of configuration coordinates  $q_e = [\theta_{je}(t), r_{te}(t), l_{re}(t), \varphi_{re}(t), \psi_{re}(t)]^T$ , used as inputs to the Inverse Dynamics block and compared with the measured parameters  $q = [\theta_j(t), r_t(t), l_r(t), \varphi_r(t), \psi_r(t)]^T$ . Comparison of predicted and measured coordinates enables us to find the deviation  $q_o = [\theta_{jo}(t), r_{to}(t), l_{ro}(t), \varphi_{ro}(t), \psi_{ro}(t)]^T$ , used as an input to the Controller block. The main function of a controller is to find the corrections  $u_o = [M_{jo}(t), F_{to}(t), F_{po}(t)]^T$  of the driving torque and forces. These correction terms are added to the

initial drive-induced excitations  $u_e = [M_{j_e}(t), F_{t_e}(t), F_{p_e}(t)]^T$ , computed in the Inverse dynamics block, yielding the values of excitations  $u = [M_j(t), F_t(t), F_p(t)]^T$  to be implemented at the given instant by the drives, in accordance with the formula:

$$\mathbf{u} = \mathbf{u}_e + \mathbf{u}_o \quad (17)$$

In order to define the structure and parameters of a MIMO controllers with five controlled quantities  $q$  and three preset ones  $u$ , it is required that differential equations be formulated, based on the Lagrange equations:

$$\frac{d}{dt} \left( \frac{\partial L}{\partial \dot{\mathbf{q}}} \right) - \frac{\partial L}{\partial \mathbf{q}} = \mathbf{u}^* \quad (18)$$

where:

$L = L(\mathbf{q}, \dot{\mathbf{q}})$  - Lagrange function for the system,

$\mathbf{u}^* = [\mathbf{u}^T, 0, 0]^T$  - matrix of generalised forces.

The system of equations (18) might be rewritten as a matrix equation [4]:

$$\mathbf{f}(\mathbf{q}, \dot{\mathbf{q}}, \ddot{\mathbf{q}}) = \mathbf{M}(\mathbf{q})\ddot{\mathbf{q}} + \mathbf{c}(\mathbf{q}, \dot{\mathbf{q}}) + \mathbf{g}(\mathbf{q}) = \mathbf{u}^* \quad (19)$$

where:

$\mathbf{M}_{5 \times 5}$  - mass matrix,

$\mathbf{c}_{5 \times 1}$  - Euler and Coriolis force matrix,

$\mathbf{g}_{5 \times 1}$  - matrix of gravity forces.

Deviations of configuration coordinates and their derivatives with respect to time can be compiled to form the state matrix  $\mathbf{z} = [\mathbf{q}_o^T, \dot{\mathbf{q}}_o^T]^T$ , thus contributing to the equation of state.

$$\dot{\mathbf{z}} = \mathbf{A}\mathbf{z} + \mathbf{B}\mathbf{u}_o, \quad \mathbf{z}(t_o) = \mathbf{z}_o \quad (20)$$

where:

$$\mathbf{A}_{10 \times 10} = \begin{bmatrix} \mathbf{0} & \mathbf{I} \\ -\mathbf{M}_e^{-1}\mathbf{K}_e & -\mathbf{M}_e^{-1}\mathbf{D}_e \end{bmatrix} \text{ - matrix of state,}$$

$\mathbf{B}_{10 \times 3}$  - control matrix.

Time - variant matrices  $M_e, K_e, D_e$  present in the matrix  $A$  are obtained by linearisation of Eq (19) in the neighbourhood of the expected values of  $q_e$ :

$$\mathbf{M}_e = \mathbf{M}(\mathbf{q}_e), \quad \mathbf{K}_e = \left. \frac{\partial \mathbf{f}}{\partial \mathbf{q}} \right|_{\mathbf{q}=\mathbf{q}_e}, \quad \mathbf{D}_e = \left. \frac{\partial \mathbf{f}}{\partial \dot{\mathbf{q}}} \right|_{\mathbf{q}=\mathbf{q}_e} \quad (21)$$

The quality criterion being taken as:

$$J = \lim_{T \rightarrow \infty} \int_0^T (\mathbf{z}^T \mathbf{Q} \mathbf{z} + \mathbf{u}^T \mathbf{I} \mathbf{u}) dt \quad (22)$$

Let us recall the Riccati equation for steady states:

$$\mathbf{H}\mathbf{A} + \mathbf{A}^T \mathbf{H} - \mathbf{H}\mathbf{B}\mathbf{I}\mathbf{B}^T \mathbf{H} + \mathbf{Q} = \mathbf{0} \quad (23)$$

where:  $\mathbf{Q}_{10 \times 10}$  - diagonal matrix of weights.

The solution to Eq (23) is a symmetrical matrix  $\mathbf{H}_{10 \times 10}$ , present in the feedback matrix  $\mathbf{K}_{3 \times 10}$ , optimal in terms of the assumed criteria of the controller:

$$\mathbf{u}_o = -\mathbf{B}^T \mathbf{H} \mathbf{z} = -\mathbf{K} \mathbf{z} \quad (24)$$

## 5. CONTROL SYSTEM PERFORMANCE

Application of the Visual Nastran 4D software yields a computational model (procedure) enabling us to preset the computed torque and forces in the drives  $\mathbf{u}$ , allowing the 'measurement' of all

components of generalised coordinates  $q$ . The Trajectory Planning, Inverse Kinematics, Inverse Dynamics and Controller blocks are implemented in Simulink environment. Both programs enable the dynamic data interchange, required to create a full simulation model of optimal control of the tower crane, shown in Fig. 3.

Simulations of optimal control of crane's drives assume a linear trajectory of the load motion, from the point  $P_s$  (29.00, 9.09, -20.00) [m] to the point  $P_f$  (11.00, 15.00, -8.00) [m]; path length  $S = 25.83$  [m]. The designed load displacement along its trajectory (Fig. 4) is governed by a polynomial function, assuming the velocity, acceleration and jerk at points  $P_s$  and  $P_f$  to be zero. The maximal load velocity is associated with the assumed time of the movement  $T = 30$  [s]. The load mass:  $m_p = 1000$  [kg], mass of the trolley:  $m_t = 50$  [kg], the mass moment of inertia of the jib and the counterweight:  $J_{zc} = 11617537$  [kgm<sup>2</sup>]. The applied matrix weights are:  $Q_{diag} = [0.05, 0.0, 0.06, 0.0, 0.05, 0.1, 0.0, 0.1, 0.0, 0.1]$ . Figs 4-6 show the plots of major simulation data. The load reached the final point with the coordinates  $P_f^*$  (10.85, 14.82, -8.09) [m], the path length approached  $S^* = 26.31$  [m], load velocity at the final point is  $0.08$  [ms<sup>-1</sup>].

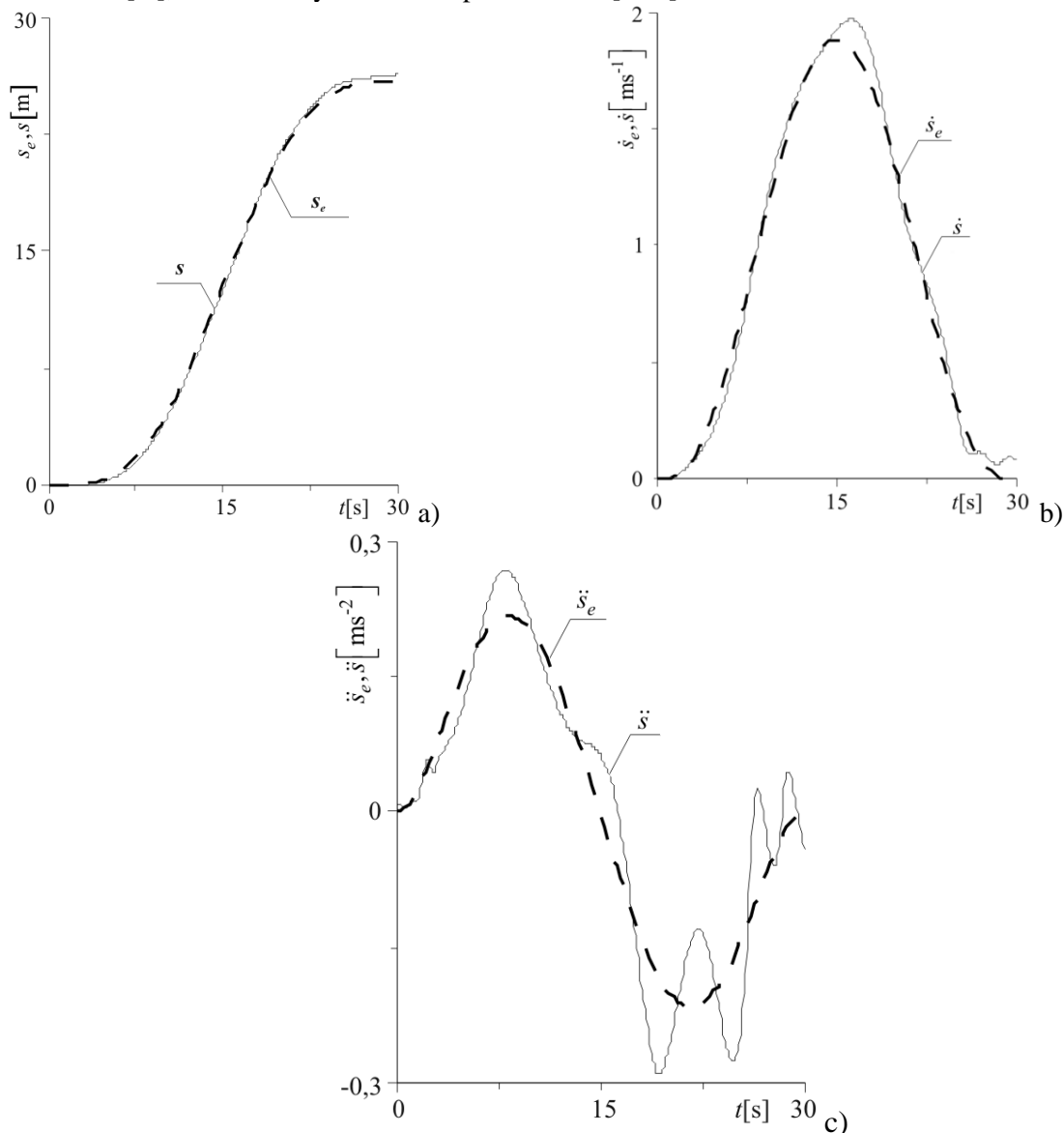


Fig. 4. Displacement and its derivatives: predicted (e-indexed) and implemented; a) displacement, b) velocity, c) acceleration

Rys. 4. Przemieszczenie i jego pochodne: przewidywane (indeks - e) i zrealizowane; a) przemieszczenie, b) prędkość, c) przyspieszenie

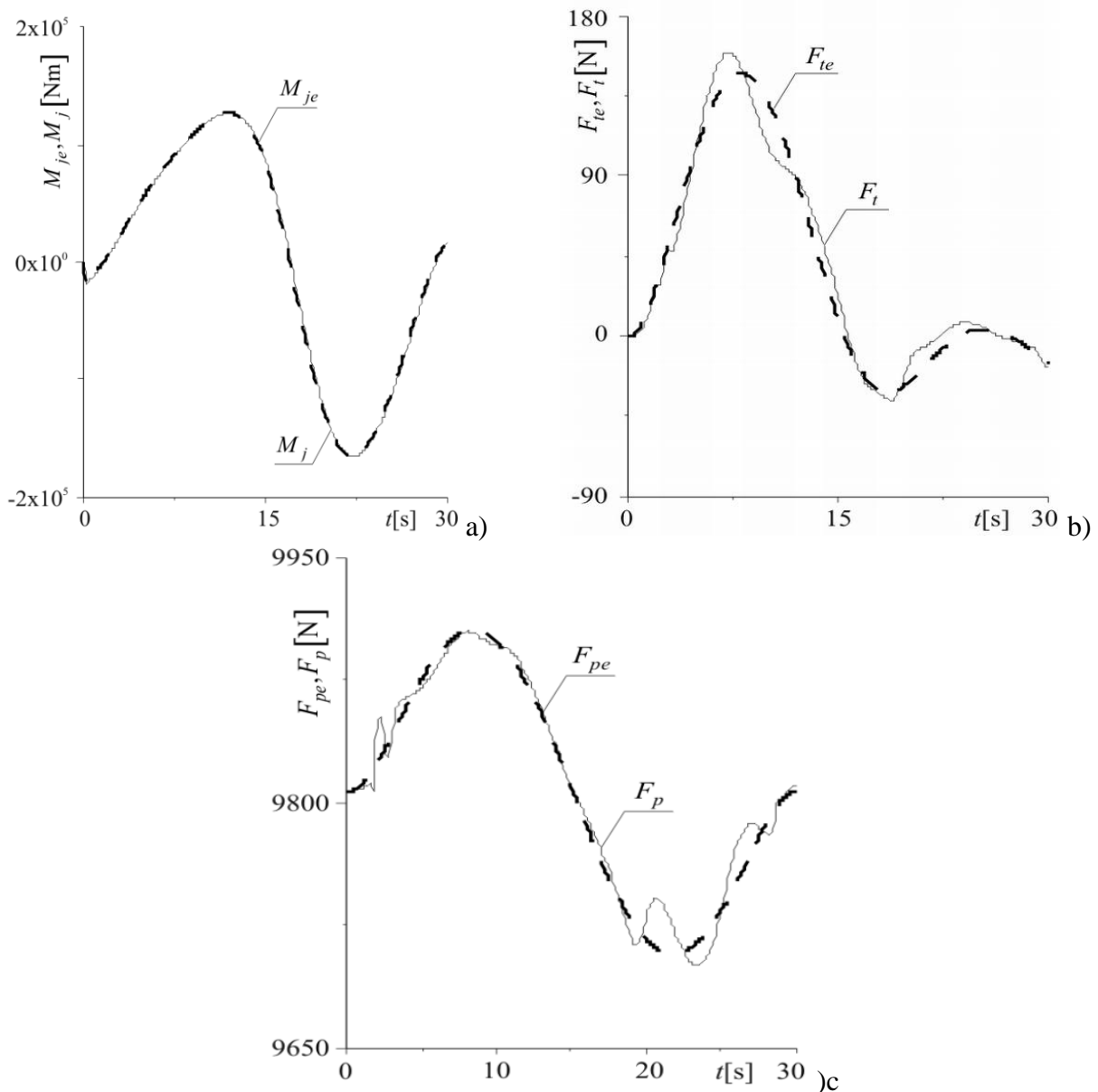


Fig. 5. Loading of the crane drives: predicted (e-indexed) and implemented; a) moment of force acting upon the jib, b) force acting upon the trolley, c) force acting upon the rope

Rys. 5. Obciążenia napędów żurawia wieżowego: przewidywane (indeks - e) i zrealizowane; a) moment napędu obrotu wysięgnika, b) siła od napędu przemieszczającego wózek, c) siła w linie

## 6. CONCLUSIONS

Simulations performed under the given assumptions confirmed the improved performance of the drive control system. The discrepancies between the pre-planned and actual trajectory are attributable to the fact that two different computer programs (Simulink, Visual Nastran 4D) were used to develop crane models used in the simulations. In order that the swing suppression system can be developed through generating the optimised trajectory, it is required that the crane model should be extended to approximate its real working conditions. The next crane model should take into account the deformations of the crane structure, rigidity and drive constraints.

The method of payload swing suppression through the synthesis of its trajectory is a practical and effective scheme in automated freight handling, where the coordinates of the end points can be

precisely determined, otherwise the method can be applied only in the systems supporting the crane operation. The end point of the payload travel path may be difficult to define because of poor visibility in the area. The operator cab is at such distance that the precise position of the payload cannot be reliably established. The desired end point of the trajectory can be also obscured by other buildings or structures, or by the payload itself. In such cases the operator needs the support of workmen stationed near the end point and equipped with the specialised devices for measuring the initial coordinates of the end point. Further corrections of the payload position are downloaded at the instant the payload approaches the workman who is to control its position. After each correction, the updated trajectory has to be calculated in real time and calculation data should be utilised for further correction of the payload position to be implemented by the crane drives.

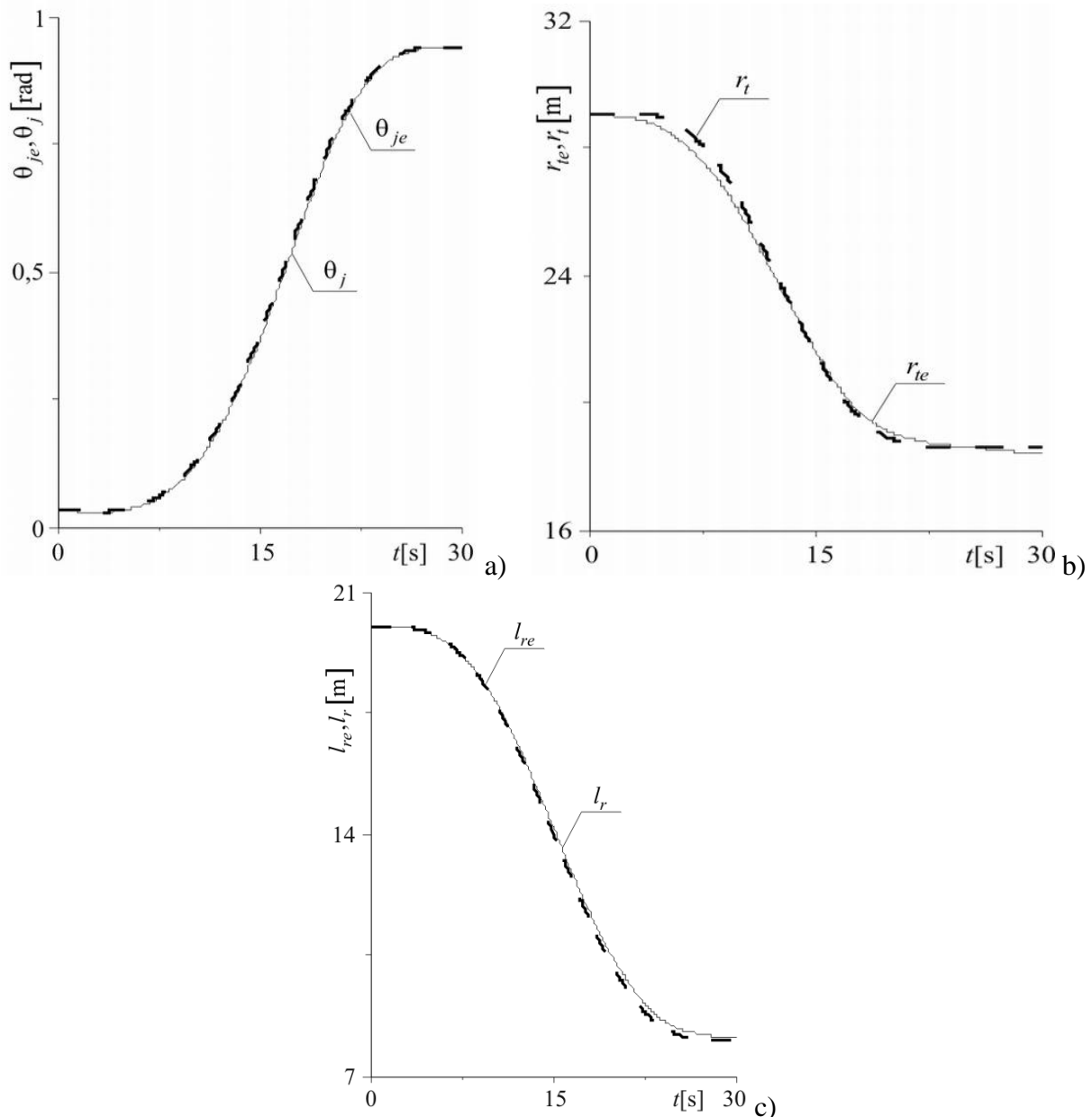


Fig. 6. Configuration coordinates: predicted (e-indexed) and implemented: a) jib rotation angle, b) distance between the trolley and the axis of rotation, c) rope length

Rys. 6. Współrzędne konfiguracyjne: przewidywane (indeks - e) i zrealizowane; a) kąt obrotu wyciągnika, b) odległość wózka od osi obrotu wyciągnika, c) długość liny

## References

1. Blackburn D., Lawrence J., Danielson J., Singhose W., Kamoi T., Taura A.: *Radial-motion assisted command shapers for nonlinear tower crane rotational slewing*. Control Engineering Practice 18 (2010), p. 523-531.
2. Ghigliazza R.M., Holmes P.: *On the dynamics of cranes, or spherical pendula with moving supports*. International Journal of Non-Linear Mechanics 37 (2002), p. 1211-1221.
3. Golafshani A.R.: *Modeling and Optimal Control of Tower Crane Motions*. A thesis presented to the University of Waterloo in fulfillment of the thesis requirement for the degree of Doctor of Philosophy in Electrical Engineering, 1999.
4. Heimann B., Gerth W., Popp K.: *Mechatronika*. PWN, Warszawa, 2001.
5. Ju F., Choo Y.S., Cui F.S.: *Dynamic response of tower crane induced by the pendulum motion of the payload*. International Journal of Solids and Structures 43 (2006), p. 376-389.
6. Kang S.C., Miranda E.: *Planning and visualization for automated robotic crane erection processes in construction*. Automation in Construction 15 (2006), p. 398-414.
7. Kłosiński J.: *Swing-free stop control of the slewing motion of a mobile crane*. Control Engineering Practice 13 (2005), p. 451-460.
8. Kozak K., Singhose W., Ebert-Uphoff I.: *Performance Measures for Input Shaping and Command Generation*. Journal of Dynamic Systems, Measurement and Control Vol. 128 (2006), p. 731-736.
9. Lawrence J.W.: *Crane Oscillation Control: Nonlinear Elements and Educational Improvements*. A Thesis Presented to The Academic Faculty In Partial Fulfillment of the Requirements for the Degree Doctor of Philosophy School of Mechanical Engineering, Georgia Institute of Technology, 2006.
10. Lee G., Kim H.H., Lee C.J., Ham S.I., Yun S.H., Cho H., Kim B.K., Kim G.T., Kim K.: *A laser-technology-based lifting-path tracking system for a robotic tower crane*. Automation in Construction 18 (2009), p. 865-874.
11. Maczynski A., Plosa J.: *Experimental verification of a method of final positioning of a load for rotary cranes*. Journal of Theoretical and Applied Mechanics 46/2 (2008), p. 443-455.
12. Sawodny O., Aschemann H., Lahres S.: *An automated gantry crane as a large workspace robot*. Control Engineering Practice 10 (2002), p. 1323-1338.
13. Solarz W., Tora G.: *Drives control of a tower crane*. Proceeding of XIX Science Conference Engineering Machines Problems, Zakopane, 2006.
14. Terashima K., Shen Y., Yano K.: *Modeling and optimal control of a rotary crane using the straight transfer transformation method*. Control Engineering Practice 15 (2007), p. 1179-1192.
15. Vaughan J.: *Dynamics and control of mobile cranes*. A Thesis Presented to The Academic Faculty In Partial Fulfillment of the Requirements for the Degree Doctor of Philosophy in the George W. Woodruff School of Mechanical Engineering, Georgia Institute of Technology, 2008.
16. Yang W., Zhang Z., Shen R.: *Modeling of system dynamics of a slewing flexible beam with moving payload pendulum*. Mechanics Research Communications 34 (2007), p. 260-266.

Received 29.05.2010; accepted in revised form 17.10.2011